PHYSICAL REVIEW B VOLUME 44, NUMBER 12 15 SEPTEMBER 1991-II

Calculated atomic structures and electronic properties of GaP, InP, GaAs, and InAs (110) surfaces

José Luiz A. Alves,* Jörk Hebenstreit,† and Matthias Scheffler
Fritz-Haber-Institut der Max-Planck-Gesellschaft, Faradayweg 4-6, D-1000 Berlin 33, Germany
(Received 11 March 1991)

We present a systematic theoretical study of several III-V semiconductor (110) surfaces based on accurate, self-consistent total-energy and force calculations, using density-functional theory and *ab initio* pseudopotentials. We study GaP, InP, GaAs, and InAs and analyze the theoretical trends for the equilibrium atomic structures, photoelectric thresholds, and surface band structures. The influence of the basis-set completeness on these results is examined. The thoeretical results are compared with experimental low-energy electron-diffraction analyses and photoemission and inverse-photoemission data.

I. INTRODUCTION

The determination and understanding of the surface atomic structure (sometimes called surface crystallography) and its relation to the surface electronic properties play a significant role in modern surface science. Low-energy electron diffraction (LEED) is the technique most frequently used in surface crystallography, but surface-extended x-ray-absorption fine structure (SEXAFS) as well as high-energy ion scattering and other techniques are also often applied. All of these techniques give *indirect* and often ambiguous information on the atomic geometry. Sometimes different techniques seem to give different results (see, for example, Ref. 1). More recently, parameter-free calculations based on the density-functional theory have been developed and such studies may become important for surface crystallography in the coming years. It appears that such *ab initio* total-energy and force calculations give a reliable description of stable and metastable atomic geometries, with uncertainties of surface geometries being less than 2% of the interatomic distances, i.e., typically less than 0.05 Å. Moreover, besides the apparent accuracy of such calculated geometries, this theory also allows an *analysis* of the obtained results to get a qualitative understanding of the mechanisms that drive the surface atoms away from the truncated bulk geometry.

In this paper we describe a systematic study of the atomic and electronic properties of several III-V (110) surfaces. In particular, we will be concerned with *trends* in the surface relaxations, surface states, and photothresholds. The latter two properties have recently attracted attention because of experimental angular-resolved photoemission and inverse photoemission studies.[2–7] These experimental results may be (and often have been) compared to calculations for the semiconductor surfaces, which are based on the density-functional theory (DFT) (Ref. 8) and the local-density approximation (LDA) for the exchange-correlation functional.[9] As we will show below, such calculated wave functions and eigenvalues depend sensitively on the atomic geometry as well as on the basis-set completeness. Thus, a high numerical accuracy in the DFT-LDA calculations is very important. Usually the eigenvalues that result from the Kohn-Sham equations are taken *directly* to interpret the surface-state energies. It is well known that such a comparison is not justified. Therefore, the calculated DFT-LDA surface-state gaps are in general too small and the occupied surface-state energies are too high above the valence band.[10] This failure in reproducing the experimental results has its roots in the improper interpretation of the DFT-LDA single-particle energy eigenvalues as the quasiparticle energies of the many-body theory.[11–14]

Recently, Zhu *et al.*[15] reported a *quasiparticle calculation* of the electron structure of GaAs(110). Their calculation is based on the Hybertsen-Louie scheme,[11] which employs perturbation theory (the so-called *GW* approximation) for the electron self-energy in order to calculate the quasiparticle energies.[16] These investigations start from the single-particle wave functions of DFT-LDA calculations using *ab initio* pseudopotentials and a slab geometry for describing the semiconductor surface. Then, the *GW* self-energy and the excitation properties of the system are evaluated. More simplified estimations give rise to somewhat larger quasiparticle corrections.[17] In order to argue about the accuracy of these results and in order to make contact with experimental data, special care has to be taken in the first step (the DFT-LDA calculation) with respect to having (i) a realistic representation of the surface geometry, (ii) a sufficiently thick slab, and (iii) a well converged representation of wave functions and electron density. In connection with the second point some discussion about the work of Zhu *et al.*[15] has appeared in the literature.[18]

In this paper we report DFT-LDA calculations using the self-consistent *ab initio* pseudopotential approach and we will address the points mentioned above. We study the GaP(110), InP(110), GaAs(110), and InAs(110) surfaces and analyze the trends for the equilibrium atomic structures, photoelectric thresholds, and surface band structures.

II. THEORETICAL FRAMEWORK

We use the density-functional theory together with the local-density approximation for the exchange-correlation functional.[8,9] The electron-gas data for the LDA are taken from Ceperley and Alder[19] as parametrized by Perdew

and Zunger.[20] The electron-ion interaction is described by norm-conserving, fully separable *ab initio* pseudopotentials.[21,22] They are based on relativistic all-electron calculations for the free atom by solving the Dirac equation self-consistently.[23,25]

In order to describe the surfaces we use the slab supercell method.[26] Each slab consists of eight atomic (110) planes. The lattice constants are fixed at the theoretical equilibrium values, and are given for the four systems in Table I. The theoretical lattice constants (including the effects of zero-point motion) are about 1–2 % smaller than the experimental ones. These discrepancies have been attributed to the missing contribution of the Ga $3d$ and In $4d$ states, which are considered as frozen-core states and thus hidden in the pseudopotentials.[27] We used vacuum regions with a thickness equivalent to six atomic layers. These choices have been proven to be adequate for describing the bulk region and for minimizing the interaction between contiguous surfaces. Figure 1 shows the electrostatic potential, $V_{es}=V_H+V_{ion}^{local}$, and the potential $\tilde{V}_{eff}=V_{es}+V_{xc}$ (V_H is the Hartree potential, V_{xc} is the exchange-correlation potential, and V_{ion}^{local} contains the local part of the pseudopotential), averaged parallel to the surface as a function of the distance z from the surface. The figure shows that both potentials are already bulklike in the third layer and reach the same value in the vacuum region. The latter result indicates that the vacuum region is large enough to permit the full decay of the electron density. In these, as well as in all the other calculations presented below, the central two layers of the slab were kept fixed at the bulk positions and the three outermost layers of atoms on both sides of the slab were relaxed to geometries given by the calculated total energies and forces. The equilibrium geometry is identified when all forces are smaller than 0.005 eV/Å. This corresponds to a *numerical* uncertainty in atomic position of less than 0.05 Å. The single-particle orbitals for the valence electrons were expanded in plane waves using basis sets with cutoffs in the kinetic energy $(\mathbf{k}+\mathbf{G})^2$ equals to 8 and 18 Ry. These basis sets will be discussed in the following section. The summation over four Monkhorst-Pack[28] $\mathbf{k}$ points in the irreducible part of the surface Brillouin zone was used to replace the Brillouin-zone integrations.

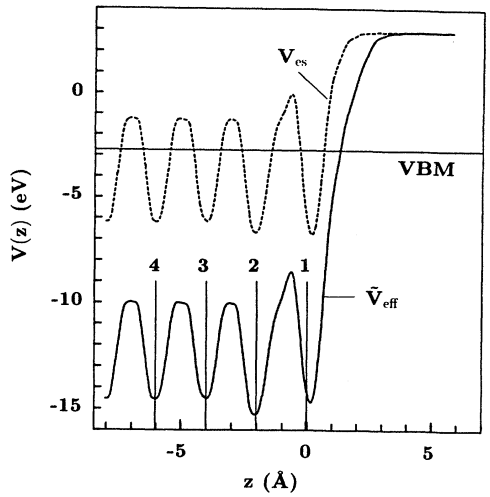

FIG. 1. Electrostatic potential (dashed line) and effective potential (solid line) for the slab used to represent the InP(110) surface with an 8-Ry cutoff. The potentials were averaged parallel to the surface and plotted as a function of distance z from the surface. The vertical bars show the ideal position of the atomic layers.

III. BASIS SET (PART 1)

We used plane-wave basis sets to expand the single-particle orbitals for the valence electrons. One problem connected with a plane-wave basis expansion is the slow

TABLE I. Structural parameters for the surface relaxation as defined in Fig. 3. The changes of the cation-anion distances (labeled c_ia_j) between neighboring atoms in the first two layers ($i,j=1$ or 2) of our slab are given in the last three columns. In the first line, for each compound, results from experimental analyses are given (Refs. 37 and 38). The data in the second and third lines correspond to cutoffs of 8 and 18 Ry, neglecting effects of zero-point motion.

	a_0 (Å)	$\Delta_{1,\perp}$ (Å)	$\Delta_{1,x}$ (Å)	$\Delta_{2,\perp}$ (Å)	$d_{12,\perp}$ (Å)	$d_{12,x}$ (Å)	ω (deg)	Bond-length change (%) c_1a_1	c_2a_1	c_1a_2
GaP	5.450	0.63	4.242	0.080	1.386	3.196	27.5	0.00	−3.75	
	5.363	0.57	4.278	0.082	1.393	3.046	27.8	−2.72	−0.10	−2.49
	5.359	0.61	4.259	0.096	1.373	3.062	29.2	−1.94	+0.03	−2.16
InP	5.869	0.73	4.598	0.140	1.549	3.382	29.9	−0.03	−0.49	
	5.678	0.64	4.526	0.110	1.447	3.241	29.2	−2.47	−0.04	−2.28
	5.662	0.67	4.517	0.117	1.435	3.216	30.1	−1.78	−0.23	−1.89
GaAs	5.654	0.69	4.518	0.120	1.442	3.339	31.1	−1.95	−0.49	
	5.500	0.63	4.355	0.090	1.460	3.145	28.6	−1.55	+1.27	−1.34
	5.559	0.67	4.407	0.098	1.415	3.190	30.2	−1.34	+0.31	−2.14
InAs	6.036	0.78	4.985	0.140	1.497	3.597	36.5	−4.22	+2.03	
	5.844	0.70	4.656	0.122	1.463	3.361	30.7	−1.80	−0.22	−2.00
	5.861	0.75	4.663	0.128	1.445	3.395	32.0	−1.18	−0.18	−1.82

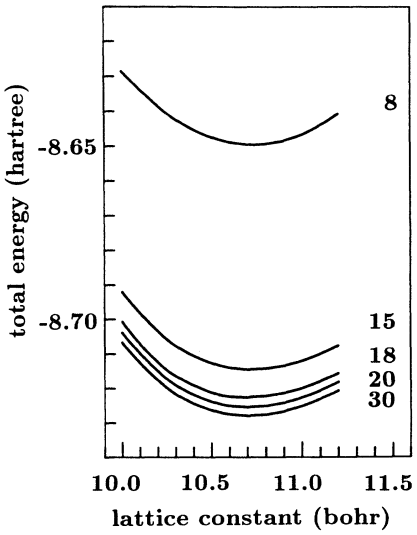

FIG. 2. Total energy per two-atom unit cell for InP with different cutoffs (running from 8 to 30 Ry) as a function of the lattice constant. For a cutoff of 18 Ry the total energy is almost converged.

convergence for some states. In order to analyze the influence of convergence of the plane-wave expansion on the atomic and electronic structures of (110) surfaces, we used basis sets with energy cutoffs of 8 and 18 Ry. In our supercell this corresponds to about 1500 and 5500 plane waves, respectively.

The energy cutoff of 8 Ry is in the range 5–10 Ry, which have been typically used in earlier surface calculations.[29–34] The 8-Ry calculations give already good results for the total-energy *differences* and thus good geometric and elastic properties. From the bulk calculation, using the 18-Ry cutoff, we also know that the total energy itself is well converged (see Fig. 2). For the surface we find a similar behavior, although here the differences in the results obtained by using basis sets with an 8- and 18-Ry cutoff are slightly more important. This is partly due to the fact that localized states require higher **k** components, and the *indirect* basis-set effects can be more important at the surface because there are more degrees of freedom for atomic displacements: the better basis set gives a slightly different surface charge density and this gives rise to forces on the atoms, and the displaced atoms give rise to different wave functions.

In the following paragraphs we will always show the results obtained for both basis sets (8- and 18-Ry energy cutoffs). A summary of the influence of the size of the basis set is given in Sec. VII.

IV. THE ATOMIC GEOMETRY

We now turn to the analysis of the equilibrium atomic geometries obtained after relaxing the III-V (110) surfaces. All surfaces relax such that the group-III surface atom moves inwards and the group-V atom moves outwards. As will be discussed later in this section, the driving mechanism for this atomic rearrangement is that under the coordination conditions of the surface, the group-III atom prefers a more planar, sp^2-like bonding situation with its three group-V neighbors and the group-V atom prefers a p bonding with its three group-III neighbors. Schematically the relaxation is shown in Fig. 3, which also defines the structural parameters that are given in Tables I and II. For the unrelaxed surface the structural parameters are as follows: the surface buckling $\Delta_{1,\perp}=0$, the second layer buckling $\Delta_{2,\perp}=0$, the distances $d_{12,\perp}$ and $\Delta_{3,\perp}$ are just the interlayer distances, and the in-plane spacing parameters are $\Delta_{1,x}=\frac{3}{4}a_0$, $d_{12,x}=\frac{1}{2}a_0$, and $\Delta_{1,\parallel}=\frac{1}{4}a_0$.

Our calculated bulk lattice constants a_0 (obtained from a bulk calculation using two special **k** points) are in all cases smaller than the experimental values. As mentioned above, this result is typical for pseudopotential calculations and has been attributed to the treatment of the d states, which are taken to be part of the ionic (frozen) potential and not as valence states.[27] Table I shows that the increasing of the basis set does not always improve the agreement with the experimental values. Again, we attribute this finding to the rough treatment of the d orbitals. If a calculation of higher accuracy is needed, then the d states would have to be treated as valence states, so that they can hybridize with other orbitals and so that the d density is treated correctly in the *nonlinear* contributions to the exchange-correlation functional. In the present work we are mainly interested in the *changes*

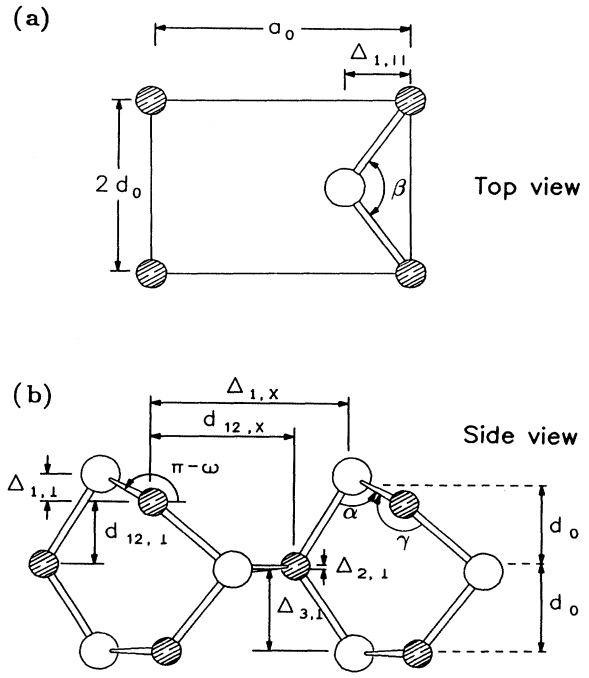

FIG. 3. Atomic geometry for III-V semiconductor (110) surfaces. (a) Top view of the surface unit cell. (b) Side view of the first three layers of the (110) surface. Open circles are anions and hatched circles are cations. a_0 is the theoretical bulk lattice constant and $d_0=\frac{1}{4}\sqrt{2}a_0$.

TABLE II. Bond angles at the anions and at the cations located at the first layer. For each compound the first line corresponds to a basis set with $E_{cut}=8$ Ry and the second to $E_{cut}=18$ Ry. For the definition of α, β, and γ see Fig. 3.

	α (deg)	β (deg)	γ (deg)
GaP	92.3	114.1	122.0
	91.0	112.1	122.9
InP	91.4	113.7	122.4
	90.4	112.5	123.2
GaAs	90.8	112.1	122.3
	90.0	111.7	123.6
InAs	90.1	112.5	123.3
	88.9	111.4	123.9

that occur at the surface. Therefore, a slightly wrong bulk lattice constant is not important (taking into account the zero-point motion, our theoretical results differ from the experimental values by about 1% for the Ga compounds and by about 2% for the In compounds).

Our results for the structural parameters are, in general, similar to those of previous calculations[35,36] and are in good agreement with low-energy electron-diffraction analysis (LEED),[37–39] as can be seen in Table I. There are some general features that we would like to emphasize.

(a) The results of LEED reveal that the III-V (110) surfaces relax with the surface cations moving inward and the surface anions being displaced outward, as shown in Fig. 3. This well-known result is reproduced by our calculations.

(b) Among the various structural parameters, the relative displacement $\Delta_{1,\perp}$ is the most accurately determined by LEED intensity analyses (to within ± 0.05 Å).[37] Our calculated values for $\Delta_{1,\perp}$ are in excellent agreement with the experimentally derived ones and this agreement improves with increasing the size of the basis set.

(c) The tile angle ω is the parameter that has been the subject of many experimental investigations.[37–39] Usually there is quite a spread for the values obtained by different experimental techniques. The experimental values quoted in Table I are those derived from the data in Ref. 37. Except for InAs our calculated values are in a good agreement with the experimental ones. We note that the tilt angle increases when the size of the basis set is increased.

(d) The calculated changes in the bond lengths of the surface atoms relative to the bulk lengths are smaller than 2.2% in the case of the 18-Ry calculation (see Table I). The changes decrease with the increase of the basis set. In the first layer of the surfaces the changes, (i.e., the cation-anion distance c_1a_1) are larger for phosphorus compounds. Our results indicate that the c_2a_1 bond length is almost unchanged whereas the c_1a_2 bond length is shortened by about 2%. Our calculated changes, in general, do not agree with those experimental values. In particular, for c_2a_1 of GaP and InAs the differences between our calculated and the experimentally obtained results are significant. At this point we suspect that these discrepancies are probably due to the fact that the LEED analyses determine $\Delta_{1,x}$ only to within approximately ± 0.2 Å and $d_{12,x}$ even less precisely.[37]

(e) The trend of the relative displacement $\Delta_{1,\perp}$ and the tilt angle ω seems to be correlated with the lattice constant when we consider the pairs of compounds with the same cations (GaP and GaAs; InP and InAs). As shown in Fig. 3, the surfaces relax in such a way that the cations move inward to an approximately planar, threefold coordination with its anion neighbors, whereas the uppermost anions move outward into a pyramidal configuration with its three cation neighbors. This relaxation has been interpreted in terms of the rehybridization of the surface bonds:[39,40] the surface As (P) changes into a more p-like configuration and the surface Ga (In) into a more sp^2-like configuration, with respect to their bulk sp^3 configuration. In this way the top-layer geometry lies between the bulk geometry (tetrahedral bonding) and the geometry obtained by putting the cation and the anion in their respective small molecule configurations, e.g., the planar GaH_3 molecule with 120° bond angles and the pyramidal AsH_3 molecule with bond angles of 92.1°, thus close to 90°.[40] In Table II we list the bond angles obtained in our calculations. As can be seen, the "pyramidal" angle α at the anion is close to 90°, the "planar" angle γ at the cation is close to 120°, and the "in-plane" angle β has values in between, close to the tetrahedral bond angle (109.47°). At the clean surface the values for α, β, and γ are that of the tetrahedral bond angle.

It has been shown that the bond angles in the trihydride molecules of group-V elements (N,P,As) increase when the bond distance is decreased because of bond repulsion.[40] We can identify a similar behavior when we consider the pairs of compounds mentioned above. When we go from the phosphorus compound to the arsenic compound the bond distance *increases,* the cation-cation repulsion *decreases,* and the pyramidal angle α *decreases.* At the same time, the *increasing* of the angle γ is facilitated. This behavior is reflected in the *increase* of the relative perpendicular displacement, $\Delta_{1,\perp}$, and in the *increase* of the tilt angle ω (see Table I). On the other hand, there is a systematic *decrease* of the angle α when the basis-set cutoff is *increased* from 8 to 18 Ry.

(f) In the second layer, the anion moves towards the bulk and the cation is pulled towards the surface. The relative displacement $\Delta_{2,\perp}$ is shown in Table I. We note that the theoretical trend is the same as the experimental one, which on the other hand follows the trend of the lattice constants.

(g) LEED analyses give bond-length-conserving, rotated top-layer structures with large displacements of the surface cations parallel to the surface of about 0.3 Å, whereas high-energy ion channeling and inverse photoemission experiments were interpreted in terms of small displacements parallel to the surface (less than 0.1 Å). Our theoretical results clearly give a large displacement of ≈ 0.3 Å for the cations, in favor of the LEED work.

V. THE PHOTOELECTRIC THRESHOLD

The photoelectric threshold is the minimum energy required to remove one electron from the valence band. In other words, it is the energy difference between the vacuum level and the valence-band maximum. Following the procedure of Ref. 29, we calculate this energy by combining bulk and surface calculations. In the bulk calculation the top of the valence band is determined relative to the bulk potential and in the surface calculation the vacuum level is determined relative to the bulk potential. Therefore by combining both calculations one is able to determine the vacuum level relative to the valence-band maximum. As we have discussed before, our slab is thick enough so that the central layers are bulklike and the vacuum region is also thick enough so that the potential saturates to the photoelectric threshold before it reaches the center of the vacuum, which separates two contiguous slabs.

Our results for the III-V compounds are shown in Table III. For the Ga and In compounds the photothreshold is decreased with increasing ionicity,[41] in agreement with the experimental trend.

The difference $\Delta_{D\text{-}L}$ between the experimental value and the calculated value for the energy cutoff of 18 Ry is a measure of how much DFT-LDA eigenvalues deviate from the true quasiparticle excitations. For the In compounds, these differences are in fair agreement with the calculated quasiparticle corrections of Bechstedt *et al.*[17] The agreement is slightly poorer for the Ga compounds. It is interesting to note that the good agreement between calculated and experimental results achieved when using the energy cutoff of 8 Ry is accidental, and it is worsened when using the better basis set with a cutoff of 18 Ry.

TABLE III. Photothresholds of III-V semiconductor compounds in units of eV.

	GaP	InP	GaAs	InAs
Expt. (Ref. 47)	6.01	5.85	5.56	5.42
8-Ry cutoff	5.79	5.69	5.43	5.50
18-Ry cutoff	5.45	5.46	5.02	5.11
Δ_{DL}	0.56	0.39	0.54	0.31

VI. THE BAND STRUCTURES

The surface band structures of the four compounds are qualitatively similar and are shown in Figs. 4–7. The solid lines indicate surface states and the labels A_i and C_i refer to wave functions localized at surface anions and cations, respectively.[42] The wave functions of the A_5 and C_3 surface states at the $\bar{M}$ point of the surface Brillouin zone are shown in Figs. 8–11. We do not show the surface states when they appear as resonances inside the projected bulk bands. The common features to all compounds are as follows.

(a) There are surface states in the fundamental gap between the valence band and the conduction band arising from both the empty cation-derived dangling bond C_3 and the occupied anion-derived dangling bond A_5 states. The effect of increasing the size of the basis set is to shift both C_3 and A_5 downward.

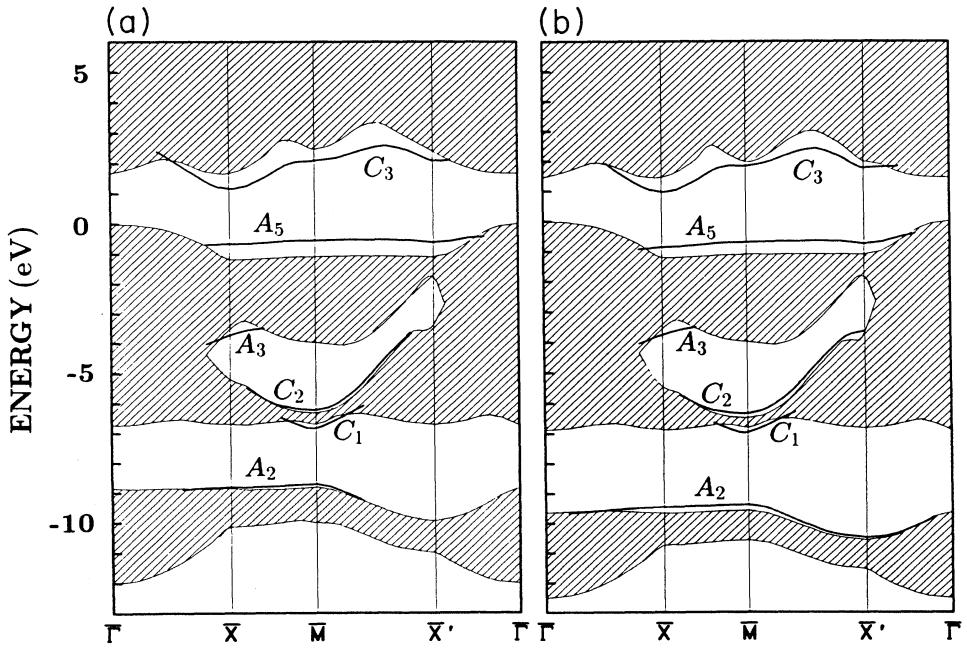

FIG. 4. Band structures for the GaP(110) surface calculated with basis-set cutoff energies of 8 Ry (left) and 18 Ry (right). The projected bulk band structures are indicated by the hatched areas. Solid lines indicate surface states and are labeled according to Ref. 39 (see text).

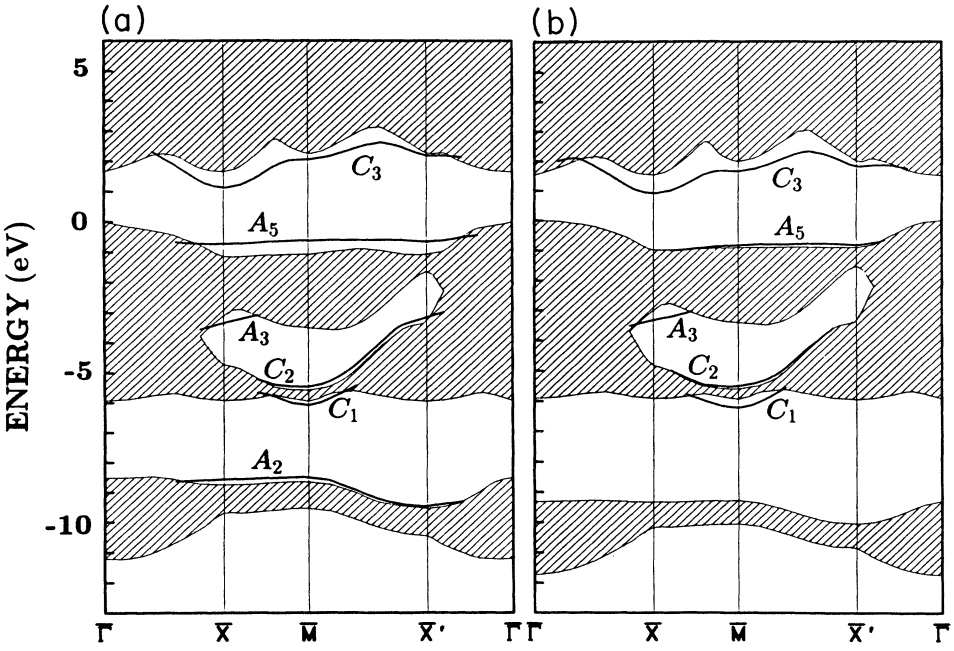

FIG. 5. Same as Fig. 4 but for the InP(110).

(b) The surface-state gaps ΔE_s increase in the order $\Delta E_s(\bar{X}) < \Delta E_s(\bar{M}) \leq \Delta E_s(\bar{X}')$.

(c) There are surface states A_3 (p_x-like) and C_2 (s-like) lying in the central region of the bulk valence bands (stomach gap) that show strong dispersion; the positions of these states are not influenced very much by the size of the basis set.

(d) There are s-like surface states A_2 lying in the lower part of bulk valence-band gap (≈ -9.0 eV). These states can be shifted downward by as much as 0.8 eV when increasing the basis set.

(e) There are s-like surface states C_1 in the heteropolar band gap. They appear around the point $\bar{M}$, at ≈ -6.5 eV, show strong dispersion, and are not influenced very

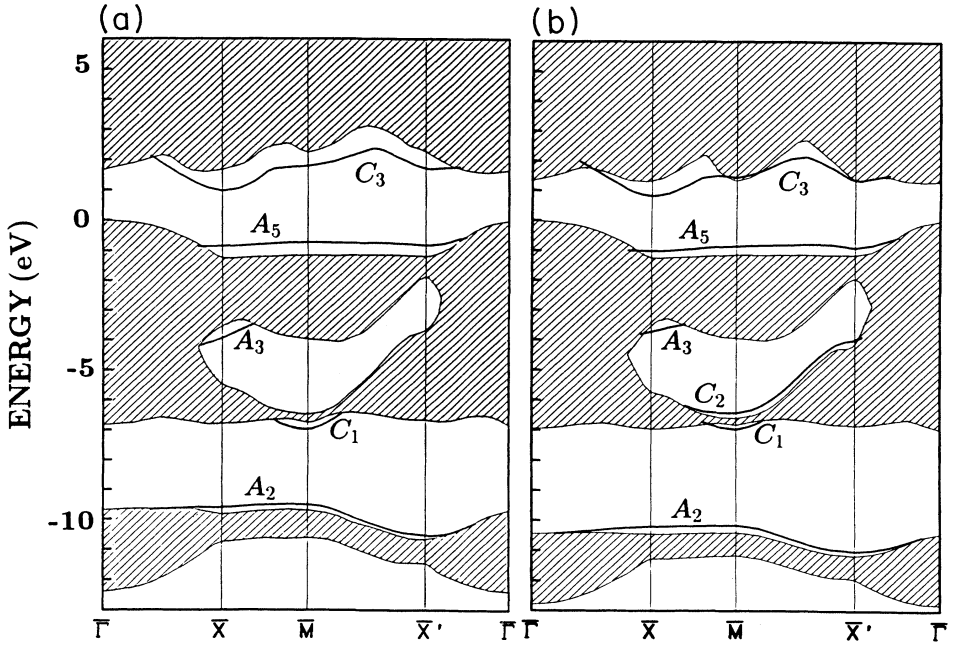

FIG. 6. Same as Fig. 4 but for the GaAs(110).

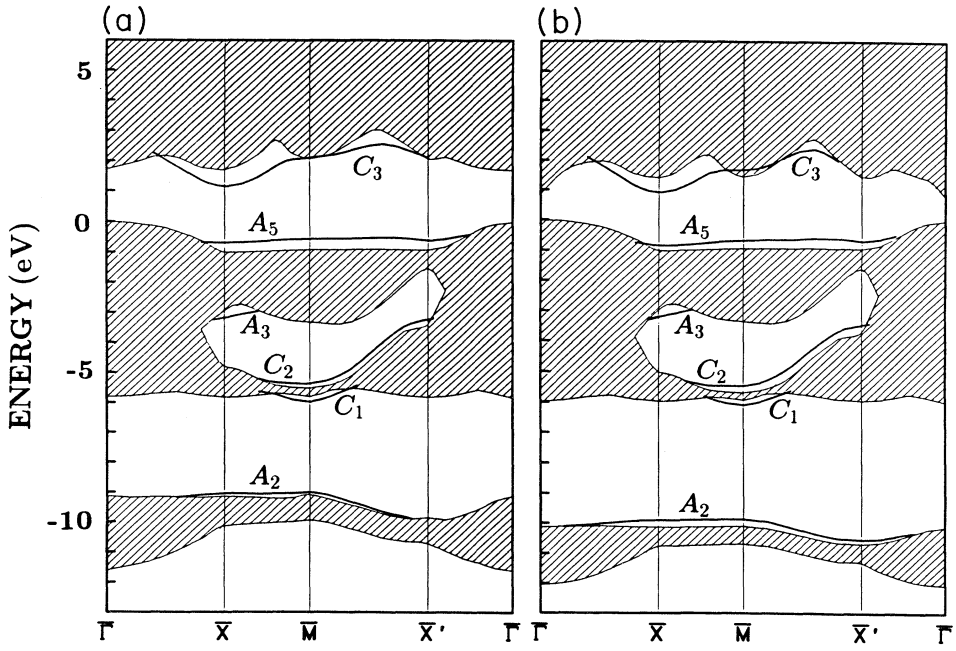

FIG. 7. Same as Fig. 4 but for the InAs(110).

much by the size of the basis set.

(f) Comparing Fig. 4 with Fig. 5 and Fig. 6 with Fig. 7 we see some correlation between the band structures and the ionic character of the compounds upon the exchange of the cations: the lower *s* band and the bottom of the *sp* band shift upward relative to the valence-band maximum, such that the heteropolar gap increases.

Experimental information concerning the energy position of surface states can be extracted from direct and inverse photoemission, and from electron-energy-loss spectroscopy. In Table IV we have compiled a list of experimental data for the energy positions of the surface states we have described above. The discrepancies between calculated and experimental values are to be attributed to the many-body corrections to the DFT-LDA results. If one considers the results of the calculations of Zhu *et al.*[15] for GaAs(110), an average many-body correction to the DFT-LDA eigenvalues for the C_3 state of about $+0.6$ eV and for the A_5 state of about -0.3 eV is to be expected. Such corrections would bring our LDA results into fair agreement with the experimental results for GaAs(110). In this connection we would like to compare our results with the recent surface-state gap measurements of Cartensen *et al.*[2] Combining angular-resolved photoemission and inverse photoemission they measured the surface-state gaps for the surfaces considered in our work. Once again, based on the work of Zhu *et al.*[15] for GaAs(110), an average many-body correction of ≈ 0.9 eV would bring our results into fair agreement with their measured gaps. We note, however, that the experimental ordering $\Delta E_s(\bar{\Gamma}) < \Delta E_s(\bar{X}') < \Delta E_s(\bar{X}) < \Delta E_s(\bar{M})$ for the surface-state gaps obtained by Cartensen *et al.*[2] is not the same as that predicted by our DFT-LDA calculations. We obtain $\Delta E_s(\bar{X}) < \Delta E_s(\bar{M}) \leq \Delta E_s(\bar{X}')$, and are unable to identify unambiguously the surface states at $\bar{\Gamma}$ because both surface states are buried in the valence or conduction band. Although Cartensen *et al.*[2] assert that the experimental errors are about ± 0.05 eV for $\bar{X}$ and $\bar{X}'$ and about ± 0.15 eV for $\bar{\Gamma}$ and $\bar{M}$, we suspect that these errors can be larger, at least at the $\bar{\Gamma}$ and $\bar{M}$ points. In particular, we see in the published spectra[2] that they may have the same difficulty at $\bar{\Gamma}$ as we have.

Our results are qualitatively in agreement with other theoretical findings of previous slab pseudopotential calculations. Most of these earlier calculations used semiempirical pseudopotentials, the experimentally inferred atomic geometries, and employed the X_α approximation for the exchange-correlation term.[30–33,42–44] Only the calculations by Zunger,[34] Zhang and Cohen,[31] and Qian, Martin, and Chadi[29] may be compared with our *ab initio* study. All these studies refer to the GaAs(110) surface. Zunger[34] used slabs formed by nine layers of atoms separated by six layers of vacuum and the LEED-derived[45] surface atomic geometry. He considered the energy cutoff of 4.1 Ry extended to 9.5 Ry by the second-order Löwdin perturbation technique.[46] Contrary to our results, he did not find any unoccupied state in the gap and did not predict any surface state in the heteropolar gap. Zhang and Cohen[31] used basis sets with $E_{\rm cut}=5$ Ry and $E_{\rm cut}=10$ Ry (where $E_{\rm cut}$ represents the kinetic-energy cutoff), slabs of eleven atomic layers separated by vacuum regions of four such layers, and the experimentally derived geometry of Mailhiot *et al.*[37] They predict smaller surface-state gaps than we. Qian, Martin, and Chadi[29] used soft *ab initio* pseudopotentials, slabs made

of five layers of atoms separated by three layers of vacuum, and an energy cutoff of 6 Ry. They determined the surface geometry of GaAs(110) from their calculation, similar to the way we have obtained it. However, their atomic geometries are different from ours (e.g., they obtained $\Delta_{1,\perp}=0.58$ Å and $\omega=27.4°$) and their calculated photothreshold is 4.94 eV. We believe that these differences are due to the fact that their slab, as well as their vacuum region, are smaller than ours. This gives rise to a stronger surface-surface interaction.

In Figs. 8–11 we show the anion and cation dangling-bond states (A_5 and C_3) for the four studied compounds. The A_5 band is filled whereas the C_3 band is empty. The right panels of Figs. 8–11 show the "good basis-set" results ($E_{\rm cut}=18$ Ry). All the anion states look very much like p states at the surface atoms and all have an important sp^3-hybrid component at the anion in the third layer. They look very similar for all compounds; even between the As and P dangling bonds the differences are not substantial. The cation dangling-bond states are more extended and their density maxima are smaller compared to the anion dangling-bond states. They reflect a strong mixing of s and p orbitals.

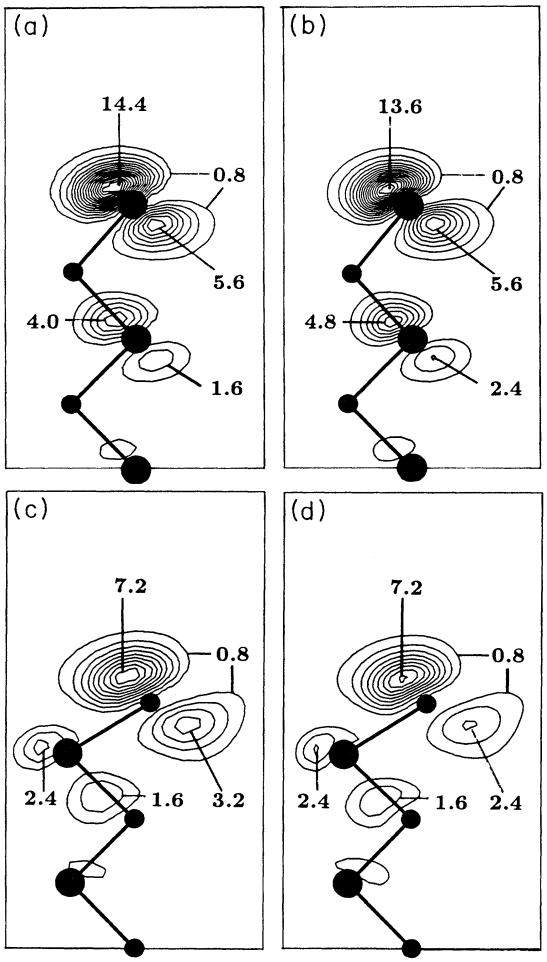

FIG. 8. Charge densities of the two surface states in the fundamental band gap at the $\bar{M}$ point of the surface Brillouin zone for GaP. The upper part shows the anion dangling orbital, i.e., the A_5 state, and the lower part shows the cation dangling orbital, i.e., the C_3 state. The left panels are obtained using a basis set with $E_{\rm cut}=8$ Ry and the right panels are obtained with a basis set of $E_{\rm cut}=18$ Ry. Small circles indicate the cations and big circles indicate the anions. Units are 10^{-3} bohr^{-3}.

VII. BASIS SET (PART 2)

In this section we summarize the influence of the size of the basis set on quantitative results. Fortunately no *qualitative* changes occur when we increase the basis set from $E_{\rm cut}=8$ Ry to $E_{\rm cut}=18$ Ry. In short we observe the following.

(1) With respect to the *surface geometry* (see Table I) we find (a) the tilt angle ω *increases* by $\approx 1°$; (b) the first-layer buckling $\Delta_{1,\perp}$ *increases* by ≈ 0.07 Å; and (c) the second-layer buckling $\Delta_{2,\perp}$ *increases* by ≈ 0.01 Å.

(2) With respect to the *band structure* (see Figs. 4–7) we find (a) the main effect is that all the energy bands

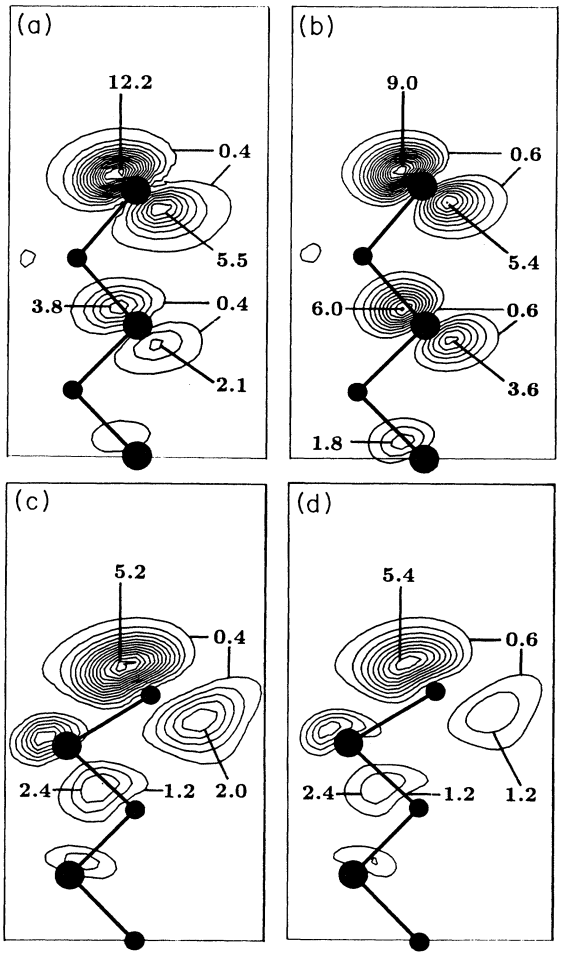

FIG. 9. Same as Fig. 8 but for InP.

move down relative to the top of the valence band; (b) the heteropolar band gap *increases* by ≈ 0.7 eV; (c) the width of the *s* band *decreases* by ≈ 0.15 eV; (d) the width of the *sp* valence band *increases* by ≈ 0.1 eV; (e) the fundamental band gap *decreases* by ≈ 0.3 eV; (f) the surface-state gap *decreases* by ≈ 0.2 eV; (g) the different surface states shift by different amounts. Changes can be as large as 0.6 eV and depend on the $\mathbf{k}_{\parallel}$ vector.

(3) The *photoelectric threshold* (compare Table II) *decreases* by ≈ 0.3 eV.

(4) For the surface states, as can be seen in Figs. 8–11, significant changes occur for some materials (e.g., InP and GaAs). A general behavior is that when the occupied surface state A_5 gets close to the valence band as a result of the increase of the basis set, the charge tends to "leak" to the bulk, as can be inferred from the charge densities shown in Figs. 8–11 and the band structures shown in Figs. 4–7. A similar behavior is observed for the unoccupied state C_3 with regard to the conduction band. When going from an 8- to an 18-Ry cutoff the shape of the corresponding orbitals is changed slightly. In the 8-Ry calculation they look purely *p*-like whereas in the 18-Ry calculation they are more localized at the vacuum side of the surface. At the same time the states get more bulk contributions (except for InP, where the trend is the opposite one). This can be seen especially for GaAs and InAs (Figs. 10 and 11). The reason for this behavior is that the unoccupied states become resonant with the conduction band at the $\bar{M}$ point (compare Figs. 6 and 7).

VIII. SUMMARY

We have reported parameter-free calculations of the surface crystallography and electronic structure of various III-V compounds, namely GaP(110), InP(110), GaAs(110), and InAs(110). We stress the influence of a good basis set, which is more important for a proper description of the surface electron density and surface states than for the bulk. The top three layers of our surfaces are relaxed according to the forces on the atoms, using an "optimized steepest descent" method together with a Car-Parrinello[52] approach for bringing the wave functions to self-consistency. For the GaAs(110) surface our calculated atomic geometries support the results of LEED analyses and the quantitative differences of the bond lengths *changes* between LEED and our parameter-free approach are in fact smaller than 1% of

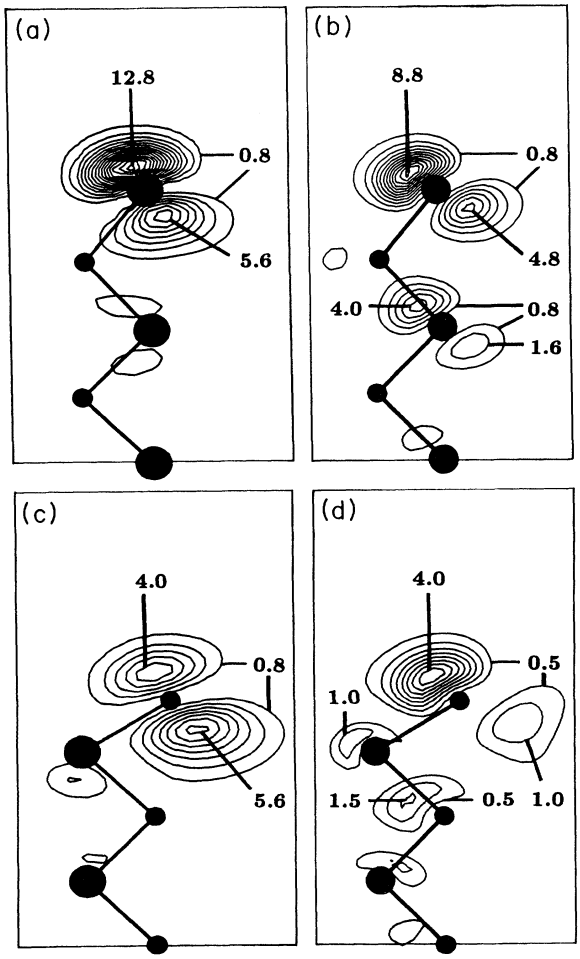

FIG. 10. Same as Fig. 8 but for GaAs.

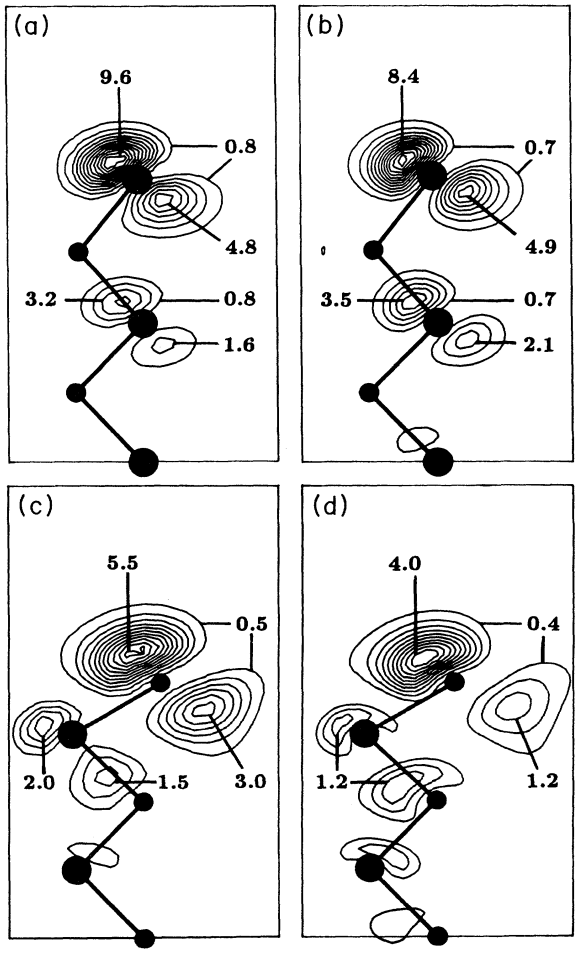

FIG. 11. Same as Fig. 8 but for InAs.

TABLE IV. Energy positions of calculated surface features (the corresponding $\mathbf{k}_{\parallel}$ point is given in parentheses) referred to the top of the valence band. The notation is as in Figs. 4–7. The data in the first and second lines, for each compound, correspond to cutoffs of 8 and 18 Ry, respectively. The third (and fourth) line shows experimentally determined positions. All energies are in eV.

	$C_3(\bar{X})$	$A_5(\bar{X})$	$A_{3a}(\bar{X})$	$C_2(\bar{M})$	$C_1(\bar{M})$	$A_2(\bar{X})$
GaP	1.16	−0.68	−3.73	−6.24	−6.84	−8.72
	0.97	−0.93	−3.76	−6.34	−6.96	−9.47
	1.70[a]	−1.2[a]		−6.5[a]	−6.5[a]	−10.5[a]
InP	1.14	−0.72	−3.33	−5.46	−6.09	−8.50
	0.92	−0.82	−3.32	−5.46	−6.21	−9.30
	1.45[a]	−1.2[a]; −0.8[b]		−5.8[a]	−5.8[a]	−9.3[a]
GaAs	0.93	−0.89	−3.87	−6.44	−7.00	−9.65
	0.83	−1.02	−3.73	−6.42	−6.97	−10.1
	1.4[a]	−1.2[a]	−3.7[c]	−6.6[a,c]; −7.0[d]	−6.6[a,c]; −7.0[d]	−10.4[a]; −11.0[e]
	1.70[f]	−1.3[g]				−11.0[c]
InAs	1.15	−0.68	−3.18	−5.36	−6.00	−9.00
	0.92	−0.85	−3.21	−5.46	−6.09	−9.90
	1.2[a]	−1.2[a]		−5.8[a]	−5.8[a]	−9.0[a]

[a]Reference 47.
[b]Reference 43.
[c]Reference 49.
[d]Reference 51.
[e]Reference 50.
[f]Reference 4.
[g]Reference 48.

the bond lengths. For GaP and InAs these differences, however, are more pronounced (see, for example, $c_1 a_1$ in Table I), i.e., between 2% and 3%. Our numerical error bars are less than ±1%. Of course, possible LDA-induced errors and the use of the frozen-core approximation will give some additional errors. Based on experience for molecules and bulk calculations, it is generally believed that for calculated *changes* of atomic geometries these contributions are very small. Therefore additional LEED studies for these two systems would be important.

We also present results of photothresholds for the four (110) surfaces, finding reasonable agreement with experimental results. The differences between theoretical and experimental results are of the order of 0.4 eV for the In compounds and 0.2 eV for the Ga compounds. These differences are due to the DFT-LDA theory as well as due to the fact that the In 4*d* and the Ga 3*d* orbitals are treated as frozen core states.

All studied compounds have surface states in the fundamental band gap: the highest occupied state, A_5, which is localized at the anions, and the lowest unoccupied state, C_3, which is localized at the cations. The $\mathbf{k}_{\parallel}$ dependence of the A_5-C_3 gap is discussed. If we take the result for GaAs(110) (Ref. 15) that the difference between DFT-LDA eigenvalues and the corresponding electronic excitations are independent of $\mathbf{k}_{\parallel}$, and if we assume that this would also hold for GaP, InP, and InAs, we find a different trend of the surface-state gap to that of a recent experimental study.[2] This difference may indicate that the assumption of a $\mathbf{k}_{\parallel}$-independent correction is incorrect or that the experimental identification of the two surface states at $\bar{\Gamma}$ and $\bar{M}$ is incorrect. At this point we are unable to judge between these two possibilities.

ACKNOWLEDGMENT

One of the authors (J.L.A.A.) acknowledges the Brazilian agency Coordenação de Aperfeiçoamento de Pessoal de Nivel Superior (CAPES) for partial support of this work.

*Permanent address: Universidade Federal de Minas Gerais, Instituto de Ciências Exatas, Departamento de Fisica, Caixa Postale 702 Belo Horizonte, Brazil.
†Permanent address: Friedrich-Schiller-Universität Jena, Institut für Festkörpertheorie und Theoretische Optik, Max-Wien-Platz 1, O-6900 Jena, Germany.

[1]C. B. Duke and A. Paton, Surf. Sci. **164**, L797 (1985).
[2]H. Cartensen, R. Claessen, R. Manzke, and M. Skibowski, Phys. Rev. B **41**, 9880 (1990).
[3]R. Haight and J. A. Silberman, Phys. Rev. Lett. **62**, 815 (1989).
[4]B. Reihl, T. Riesterer, M. Tschudy, and P. Perfetti, Phys. Rev. B **38**, 13 456 (1988).
[5]T. Riesterer, P. Perfetti, M. Tschudy, and B. Reihl, Surf. Sci. **189/190**, 795 (1987).
[6]D. Straub, M. Skibowski, and F. J. Himpsel, Phys. Rev. B **32**, 5237 (1985).
[7]D. Straub, M. Skibowski, and F. J. Himpsel, J. Vac. Sci. Technol. A **3**, 1484 (1985).
[8]P. Hohenberg and W. Kohn, Phys. Rev. **136**, B864 (1964).
[9]W. Kohn and L. J. Sham, Phys. Rev. **140**, A1133 (1965).
[10]S. G. Louie, in *Electronic Structure, Dynamics and Quantum Structural Properties of Condensed Matter*, edited by J. Devreese and P. van Camp (Plenum, New York, 1985), p. 335.
[11]M. S. Hybertsen and S. G. Louie, Phys. Rev. B **34**, 5390

(1986); **38**, 4033 (1988).
[12]R. Godby, M. Schlüter, and L. J. Sham, Phys. Rev. B **37**, 10 159 (1989).
[13]W. von der Linden and P. Horsch, Phys. Rev. B **37**, 8351 (1988).
[14]F. Bechstedt and R. Del Sole, Phys. Rev. B **38**, 7710 (1988).
[15]Xuejun Zhu, S. B. Zhang, S. G. Louie, and M. L. Cohen, Phys. Rev. Lett. **63**, 2112 (1989).
[16]L. Hedin, Phys. Rev. **139**, A796 (1965); L. Hedin and S. Lundqvist, in *Solid State Physics,* edited by F. Seitz, D. Turnbull, and H. Ehrenreich (Academic, New York, 1969), Vol. 23, p. 1.
[17]F. Bechstedt, R. Del Sole, and F. Manghi, J. Phys. Condens. Matter **1**, SB75 (1989); F. Bechstedt and R. Del Sole, Solid State Commun. **74**, 41 (1990).
[18]F. Manghi, E. Molinari, A. Selloni, and R. Del Sole, Phys. Rev. Lett. **65**, 937 (1990); Xuejun Zhu, S. B. Zhang, S. G. Louie, and M. L. Cohen, *ibid.* **65**, 938 (1990).
[19]D. M. Ceperley and B. I. Alder, Phys. Rev. Lett. **45**, 566 (1980).
[20]P. Perdew and A. Zunger, Phys. Rev. B **23**, 5048 (1981).
[21]*A list of separable, norm-conserving, ab-initio pseudopotentials,* Fritz-Haber-Institut Research Report 1990 (unpublished).
[22]X. Gonze, P. Käckell, and M. Scheffler, Phys. Rev. B **41**, 12 264 (1990).
[23]D. R. Hamann, M. Schlüter, and C. Chiang, Phys. Rev. Lett. **43**, 1494 (1979).
[24]G. B. Bachlet, D. R. Hamann, and M. Schlüter, Phys. Rev. B **26**, 4199 (1982).
[25]L. Kleinman and D. M. Bylander, Phys. Rev. Lett. **48**, 1425 (1982).
[26]M. Schlüter, J. R. Chelikowsky, S. G. Louie, and M. L. Cohen, Phys. Rev. B **12**, 4200 (1975).
[27]S. Massidda, A. Continenza, A. J. Freeman, T. M. de Pascale, F. Meloni, and M. Serra, Phys. Rev. B **41**, 12 079 (1990); G. B. Bachelet and N. E. Christensen, *ibid.* **31**, 879 (1985); N. E. Christensen, *ibid.* **37**, 4528 (1988); B. I. Min, S. Massidda, and A. J. Freeman, *ibid.* **38**, 1970 (1988); Su-Huai Wei and A. Zunger, Phys. Rev. Lett. **59**, 144 (1987); A. Continenza, S. Massidda, and A. J. Freeman, Phys. Rev. B **38**, 12 996 (1988).
[28]H. J. Monkhorst and J. D. Pack, Phys. Rev. B **13**, 5188 (1976).
[29]Guo-Xin Qian, R. M. Martin, and D. J. Chadi, Phys. Rev. B **37**, 1303 (1988).
[30]F. Manghi, C. M. Bertoni, C. Calandra, and E. Molinari, Phys. Rev. B **24**, 6029 (1981).
[31]S. B. Zhang and M. L. Cohen, Surf. Sci. **172**, 754 (1986).
[32]F. Manghi, R. Del Sole, A. Selloni, and E. Molinari, Phys. Rev. B **41**, 9935 (1990).
[33]F. Manghi, E. Molinari, C. M. Bertoni, and C. Calandra, J. Phys. C **15**, 1099 (1982).
[34]A. Zunger, Phys. Rev. B **22**, 959 (1980).
[35]D. J. Chadi, Phys. Rev. B **19**, 2074 (1979).
[36]A. C. Ferraz and G. P. Srivastava, Surf. Sci. **182**, 161 (1987).
[37]C. Mailhiot, C. B. Duke, and D. J. Chadi, Surf. Sci. **149**, 366 (1985); Phys. Rev. Lett. **53**, 2114 (1984); C. B. Duke, S. L. Richardson, A. Paton, and A. Kahn, Surf. Sci. **127**, L135 (1983).
[38]F. Bechstedt and R. Enderlein, *Semiconductor Surfaces and Interfaces* (Akademie Verlag, Berlin, 1988), and references cited therein.
[39]A. R. Lubinsky, C. B. Duke, B. W. Lee, and P. Mark, Phys. Rev. Lett. **36**, 1058 (1976); C. B. Duke, A. R. Lubinsky, B. W. Lee, and P. Mark, J. Vac. Sci. Technol. **13**, 761 (1976); A. Kahn, Surf. Sci. Rep. **3**, 193 (1983).
[40]C. A. Swarts, W. A. Goddard III, and T. C. McGill, J. Vac. Sci. Technol. **17**, 982 (1980); C. A. Swarts, T. C. McGill, and W. A. Goddard III, Surf. Sci. **110**, 400 (1981).
[41]The Phillips ionicities for GaP, InP, GaAs, and InAs are 0.374, 0.421, 0.310, and 0.357, respectively. See, for instance, Ref. 38
[42]J. R. Chelikowsky and M. L. Cohen, Solid State Commun. **29**, 267 (1979).
[43]G. P. Srivastava, I. Singh, V. Montgomery, and R. H. Williams, J. Phys. C **16**, 3627 (1983).
[44]J. R. Chelikowsky and M. L. Cohen, Phys. Rev. B **20**, 4150 (1979).
[45]S. Y. Tong, A. R. Lubinsky, B. J. Mrstik, and M. A. van Hove, Phys. Rev. B **17**, 3303 (1978).
[46]P.-O. Löwdin, J. Chem. Phys. **19**, 1396 (1951).
[47]J. van Laar, A. Huijser, and T. L. van Rooy, J. Vac. Sci. Technol. **14**, 894 (1977).
[48]A. Huijser, J. van Laar, and T. L. van Rooy, Phys. Lett. **65A**, 337 (1978).
[49]G. P. Williams, R. J. Smith, and G. J. Lapeyre, J. Vac. Sci. Technol. **15**, 1249 (1978).
[50]K. C. Pandey, J. L. Freeouf, and D. E. Eastman, J. Vac. Sci. Technol. **14**, 904 (1977).
[51]J. A. Knapp and G. J. Lapeyre, J. Vac. Sci. Technol. **13**, 757 (1976).
[52]R. Car and M. Parrinello, Phys. Rev. Lett. **55**, 2471 (1985).